High Spatial Resolution Midair Tactile Display Using 70 kHz Ultrasound

Mitsuru Ito[1]([✉]), Daisuke Wakuda[2], Seki Inoue[1], Yasutoshi Makino[1], and Hiroyuki Shinoda[1]

[1] Department of Complexity Science and Engineering,
Graduate School of Frontier Science, The University of Tokyo,
5-1-5 Kashiwanoha, Kashiwa City, Chiba, Japan
{ito,inoue}@hapis.k.u-tokyo.ac.jp,
{yasutoshi_makino,hiroyuki_shinoda}@k.u-tokyo.ac.jp
[2] Smart Life Technology Development Center,
Automotive and Industrial Systems Company,
Panasonic Corporation, 1006 Kadoma, Kadoma City, Osaka, Japan
wakuda.daisuke@jp.panasonic.com

Abstract. We fabricated a midair tactile display using a 70 kHz airborne ultrasound. The spatial resolution of the display was improved 1.75 times compared with the conventional 40 kHz ultrasound tactile display. Since the focal spot diameter was smaller than a finger pad, the user could perceive a localized spot on the finger pad. In the experiment determining the physical properties, we found that the ultrasound attenuation at 70 kHz was comparable to that at 40 kHz. The small focal spot was successfully created as expected using the theory. The psychophysical experimental results showed that the minimum perceivable radiation force for the focal spot of 70 kHz was smaller than that for the 40 kHz case in average under 40 or 100 Hz modulations, and the smaller focal spot was easier to perceive. We also conducted a comparison test of the perceived force area with real contacts.

Keywords: Midair haptics · Tactile display · Airborne ultrasound · Acoustic radiation pressure

1 Introduction

Mid-air haptic displays [1] using ultrasound [2–4] provides a convenient tool to stimulate human skins that is not wearing any device. Although the maximum force is weak, tactile sensations can be evoked at any position and time without constraining the human motions in the workspace. Such sensations can be superimposed on visual floating images [5, 6] and enables fully programmable 3D interfaces in midair [7].

However, a significant limitation of the previous midair devices was the low spatial resolution originating from the ultrasound frequency. Since the conventional devices used 40 kHz ultrasound with an 8.5 mm wavelength, the focal spot was comparable to, or larger than, a finger pad. Such spatial resolution is satisfactory in some applications but can be a critical limitation to others. Since the pressure distribution is uniform on

the finger pad, it cannot stimulate the SAI and SAII receptors effectively [8, 9]. It is impossible to display the local configuration inside the finger pad, which limits the possibility of midair handling and manipulation of floating virtual objects.

In this paper, we fabricate a 70 kHz ultrasound phased array and examine the effect of heightening the spatial resolution. Since the wavelength 5 mm is smaller than a finger pad, it can produce a localized pattern on the finger pad. The rest of the paper is organized as follows. First, we show the specification of the device. Using the device, we measure the physical properties of the generated ultrasound and confirm that high-resolution pressure distribution is achieved. As a critical property of high-frequency ultrasound, we also measure the attenuation in air and confirm the attenuation length is still acceptable for use as a tactile display. Next, we obtain the tactile threshold on a finger pad. We examine whether the smaller focus of the 70 kHz ultrasound improves the threshold for low-frequency vibration compared with the 40 kHz case. Finally, we conduct a comparison test of the perceived force area on a finger pad with real objects.

2   Basic Properties of Acoustic Radiation Pressure

The relation between the sound pressure and radiation pressure [10, 11] is summarized below for the readability of the manuscript. The acoustic radiation pressure P [Pa] is proportional to the sound energy density given by

$$P = \alpha E = \alpha \frac{p^2}{\rho c^2} \tag{1}$$

where E [J/m³], p [Pa], ρ [kg/m³], and c [m/s] denote the sound energy density, sound pressure, density of the medium, and sound velocity, respectively. α denotes a constant ranging between 1 and 2 depending on the reflection properties of the object surface. When the ultrasound propagates through the air and is blocked by the surface of an object, almost all of the ultrasound is reflected at the boundary and in this case the coefficient α becomes nearly 2. Thus, we can control the radiation pressure P by controlling the ultrasound pressure p.

The minimum diameter of the focal spot w is estimated as

$$w = 1.22 \frac{\lambda}{\sin \theta}, \quad \sin \theta = \frac{D/2}{\sqrt{R^2 + (D/2)^2}} \tag{2}$$

where λ [m] denotes the wavelength of the acoustic wave, and R [m] and D [m] denote the focal length and the diameter of the aperture, respectively [12]. The spatial resolution of the array is determined by the focal diameter w.

3   Prototype Device

We fabricated two phased arrays of 70 kHz and 40 kHz transducers with an identical arrangement as shown in Fig. 1. The device was an annular phased array with a center transducer and five additional circular layers of transducers. The prototype was
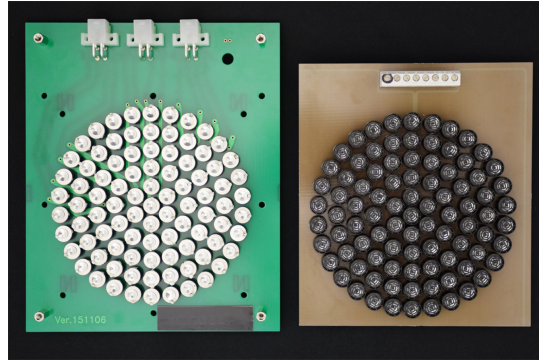
Fig. 1. Prototype devices. Left: 70 kHz phased array. Right: 40 kHz phased array. (Nihon Ceramic T4010B4)

designed to produce a single focus along the center axis perpendicular to the phased array surface. Each circle is driven at an independent phase by a real-time computer to produce a single focus. We used a commercially available 40 kHz transducers (Nihon Ceramic T4010B4) and the 70 kHz types developed for this experiment.

The external diameters of the transducers are 9 mm (70 kHz) and 10 mm (40 kHz). Figure 2(a) shows the schematic diagram of the electrical connections of the transducers. Because of the capacity of the driver IC, the 5th and 6th lines are divided into two parts. Thus, this system is driven by eight signal channels where the maximum number of the transducers connected to a single channel is 18. The output signal from the Digital I/O was amplified by a driving circuit (JRC NJM2670).

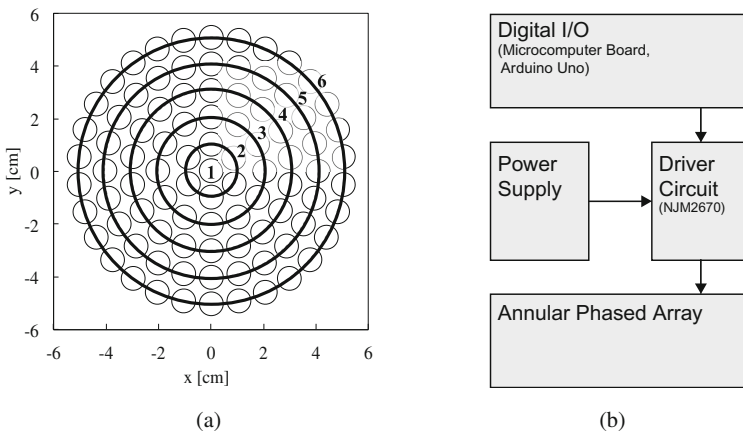The system is shown in Fig. 2. The driving signal was rectangular waves.

(a)   (b)

Fig. 2. System diagram of annular phased array. (a) Electrical connection and arrangement of transducers. (b) Block diagram of prototype system.

4 Physical Evaluation

4.1 Attenuation in the Air

A critical parameter of high-frequency ultrasound is the attenuation length. The standardized sound pressure of 70 kHz ultrasound is shown in Fig. 3. The case of 40 kHz is also plotted on the same figure. In this experiment, we used a single transmitter as the sound source. For this experiment, the amplitude difference between 40 kHz and 70 kHz ultrasound was within 10 % for the range between 100 and 500 mm. This result shows the 70 kHz ultrasound can be used in a comparable workspace to the 40 kHz case. In the following experiments, the distances between the transducer and the measurement plane are 150 mm and 300 mm.
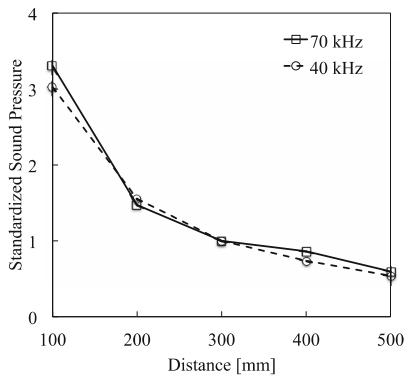

Fig. 3. Attenuation of sound pressure versus distance. The sound pressure level was measured in a range from 100 mm to 500 mm. The measurement data has been standardized by the value of the position of 300 mm. The peak-to-peak voltages of the sinusoidal driving signals at 70 kHz and 40 kHz were 70 V and 30 V, respectively.

4.2 Spatial Resolution

Figure 4 shows the experimental setup to measure the focus of the phased arrays. The phased array was mounted on an aluminum cabinet so that the transducer surface faced a standard microphone. The standard microphone (Brüel&Kjær Type 4138-A-015) with a preamplifier (Brüel&Kjær Type 2670) was mounted on a 3D stage. The diameter of the microphone head was 3.9 mm. The surface of the phased array was parallel to the x-y plane of the 3D stage composed of high-precision stages (SIGMA KOKI SGMV26-200) and a stage controller (SIGMA KOKI SHOT-304GS). The location determination accuracy of each stage was 15 μm. The data were acquired at every 1 mm. The sound signal was amplified with a power amplifier (Brüel&Kjær Type 5935) and calibrated by a sound calibrator (Brüel&Kjær Type 4321). The ultrasound was driven with a continuous rectangular signal during the measurement. Figures 5 and 6 show the spatial distribution of the measured sound pressure along the x-y plane and the x axis.
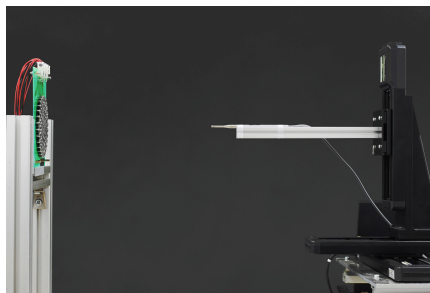
Fig. 4. Experimental setup for the measurement of the sound pressure. A microphone was attached to the 3D stage.
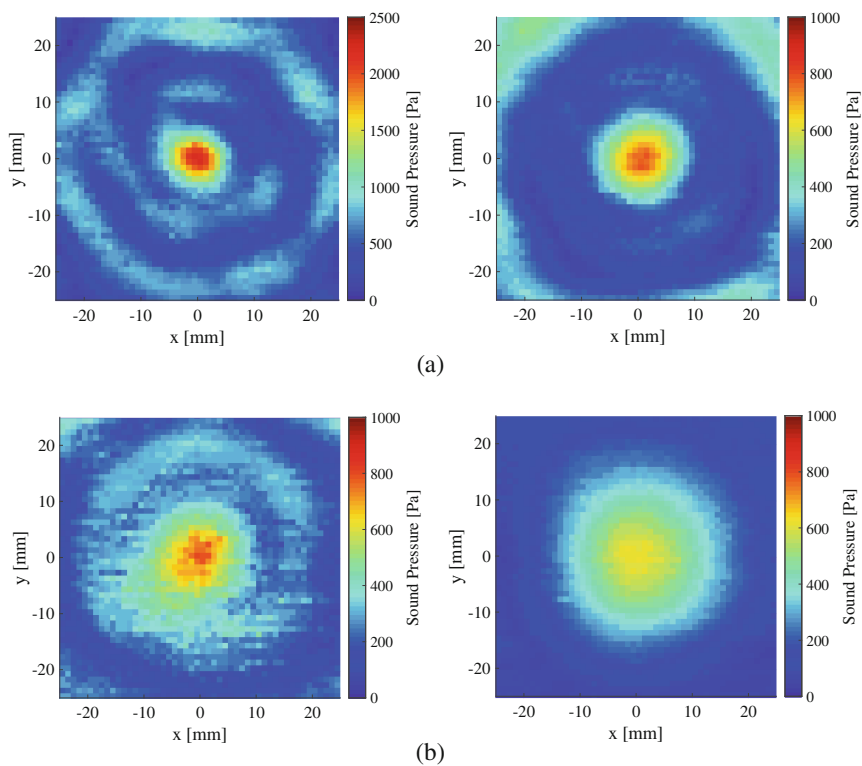

(a)

(b)

Fig. 5. Sound pressure distribution. Two dimensional spatial distribution of the sound pressure around the focus. Left: 70 kHz phased array. Right: 40 kHz phased array. (a) Focal length: 150 mm. (b) Focal length: 300 mm.
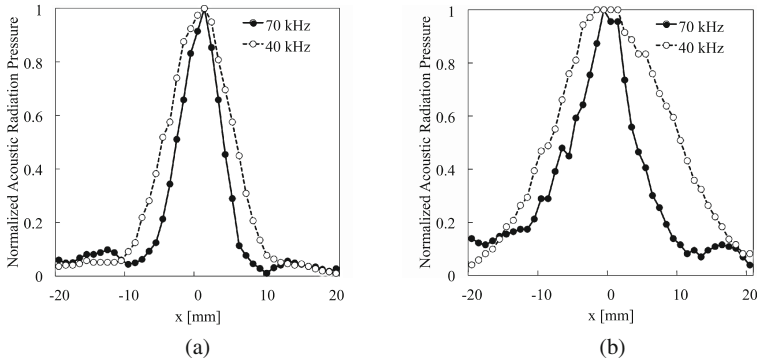
Fig. 6. Radiation pressure distribution along the line *y* = 0. (a) Focal length: 150 mm. (b) Focal length: 300 mm.

4.3   Total Force

The total force was measured using an electronic balance (ViBRA Shinko Denshi AJII-220). The strength of the stimulus in the psychophysical experiments is expressed with the total radiation force obtained in this measurement result. The surface of the phased array is parallel to the measurement plane of the electronic balance. The ultrasound was driven with a continuously rectangular wave during the measurement.

The distance between the radiation surface and the electronic balance was fixed at 150 mm. Figure 7 shows the force value at each driving voltage expressed in the peak-to-peak. In this paper's experiment, power supply to the 70 kHz phased array was 120 W.
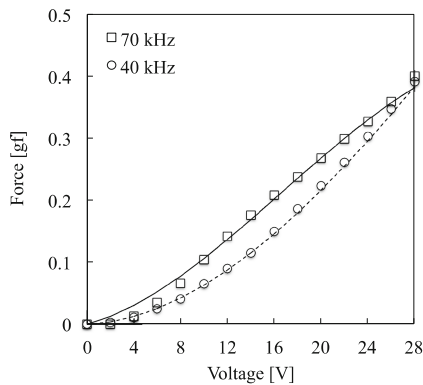

Fig. 7. Total radiation force. We used these relations to control the total acoustic power (total radiation force) from the phased array.

5   Psychophysical Experiment

In this section, we applied vibrotactile patterns to the skin surface and evaluated the threshold value of the stimulus on the finer pad. Next, we evaluated the perceived force area by comparing the stimulation with actual contact to real objects.

5.1   Amplitude Threshold

Experimental Setup and Procedure. The experimental setup is shown in Fig. 8. The experimental procedure was based on the method of limits.

The driving voltage of the phased array was varied in the range specified in Fig. 7. The stimuli were changing in 12 stages between 2 V and 24 V. The focal point was produced below the phased array center with the focal length of 150 mm. The amplitude of the ultrasound was modulated at 40 Hz and 100 Hz for both the 40 kHz and 70 kHz phased arrays. The subjects put their right-hand finger pads at the position of the focal point. The subjects wore the headphones and listened to a white noise to interrupt the audible sound from the phased array corresponding to the driving intensity. The subject gave an answer for tactile sensation on their finger pad. The subjects were allowed only two response alternatives: yes, or no. There was no time limit. The procedure included an ascending series and descending series. These pairs of series were presented three times. The procedure started with the ascending series, where a stimulus was presented at a minimum level, while the start position of descending series was at a maximum level. The subject's absolute threshold was calculated as the average of all obtained thresholds in the pairs of series. There were a total of eight subjects. All subjects were male and their ages were between 22 and 34.

Results. The results of the threshold experiment are shown in Fig. 9. The plots are the averages of the ascending and descending thresholds and the error bars here indicate the averages of the ascending and descending series. The "force" means the peak-to-peak value of the applied radiation force given as a rectangular wave.

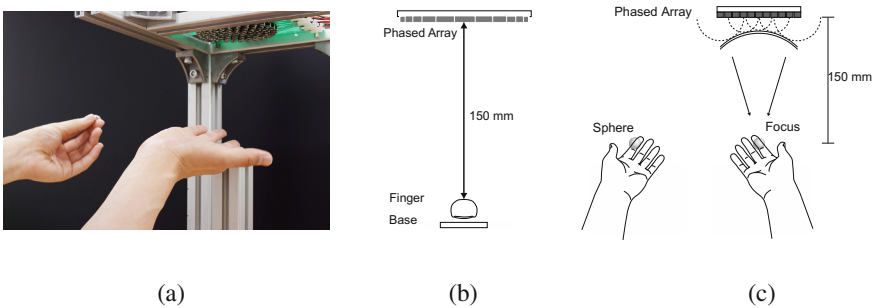| (a) | (b) | (c) |

Fig. 8. Experimental setup for the psychophysical experiments. We have set up a base for indicating the position of the finger. When the subject places the finger on the base, finger pad and the focus were in the same position.
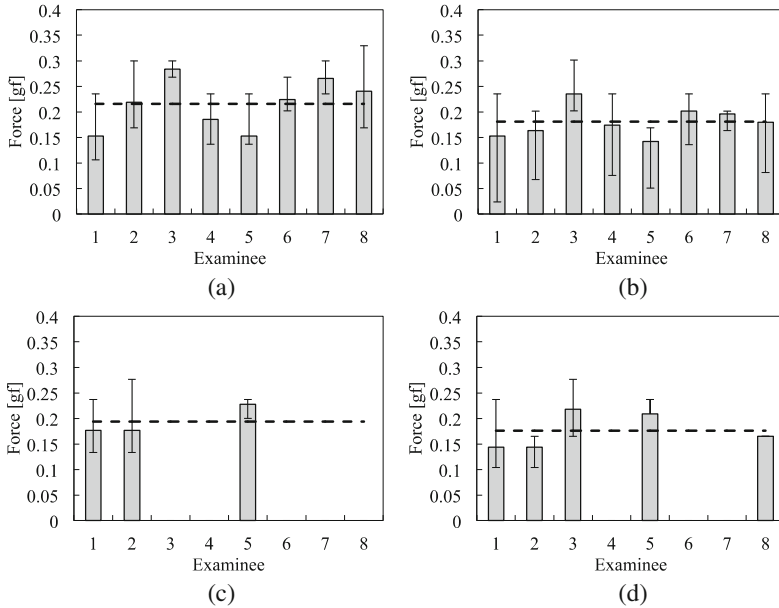
Fig. 9. Absolute detection thresholds for the focal point. (a) 70 kHz phased array, 40 Hz modulation. The average of all examinees was 0.22 gf. (b) 70 kHz phased array, 100 Hz modulation. The average of all examinees was 0.18 gf. (c) 40 kHz phased array, 40 Hz modulation. Examinee 3, 4, 6, 7, and 8 felt no sensation on their finger pad. (d) 40 kHz phased array, 100 Hz modulation. Examinee 4, 6 and 7 felt no sensation on their finger pad.

The maximum stimulus produced by the 70 kHz phased array was perceived on the finger pad for both the modulation frequency of 100 Hz and 40 Hz by all subjects. On the other hand, the maximum stimulus from the 40 kHz phased array was felt on the finger pads of only half of the subjects. Thus, we could not quantify the threshold by the 40 kHz phased array.

We also conducted a similar test for 20 Hz modulation. We did not obtain a quantitative threshold, but all of the subjects could feel the 20 Hz modulation stimulus on their finger pads for the 70 kHz phased array.

5.2   Size Comparison Test

Procedure. In this experiment, the subject compared the perceived size with real spheres for the 70 kHz focal spot. The experimental procedure was as follows. We prepared 11 stainless steel balls, which had different diameters as reference objects. Figure 10(a) shows the appearance of the reference metallic ball. The subjects, with eyes closed, have the sphere in the left hand while touching the focus with the right hand. First, the author put a reference sphere on the palm of the left hand of the subject. Then, the subjects touch the sphere freely with their fingers and compare the sphere
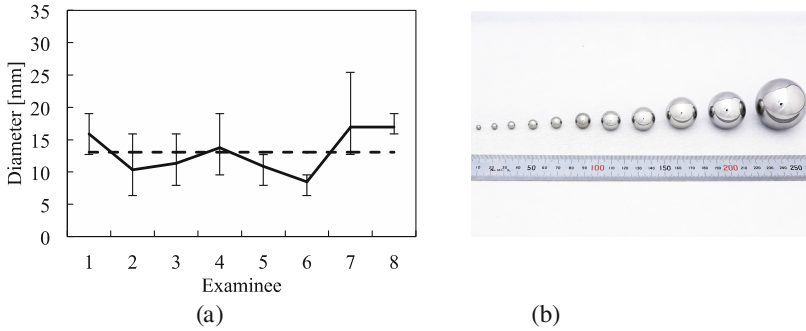
Fig. 10. (a) Perceived focus diameter. The mean value was 13.1 mm. (b) Photograph of the metal spheres used in the comparison test. The diameters of the spheres are 4, 5, 6.35, 7.93, 9.52, 12.7, 15.87, 19.05, 25.4, 30.16, and 41.27 mm.

size with the focus size. After this, the author put the next sphere on the palm of the left hand and repeat this procedure for all the kinds of spheres. All subjects were instructed to sense the stimuli at their finger pads. The subjects compared the size of the ball and the focus. The subjects were allowed multiple choices: larger, smaller, or same. There was no time limit. The experimental procedure is the method of limits similar to the threshold experiment. We started from the smallest ball, and recorded the diameter where the answer switched from the "same" to "larger", while keeping the ultrasound stimulation constant. This was used to obtain the ascending threshold. We also obtain the descending limit in a similar way. We finally obtained the equivalent diameter to the ultrasound stimulation, as the average of the ascending and descending thresholds.

Results. Figure 10 shows the equivalent sphere diameters perceived on the finger pad. In this figure, the error bars indicate the size of the maximum and minimum ball sizes which were judged as being the same as, regardless of whether in the ascending or descending process. The perceived diameter was 13.1 mm for the spot in the condition of the 70 kHz phased array.

6 Discussions

The result of Fig. 9(a), (b) shows comparable thresholds for 40 Hz and 100 Hz vibrations, which seems inconsistent with conventional knowledge. In Ref. [13], the thresholds for 40 Hz and 100 Hz are different by 15 dB for a 2.9 cm^2 contactor. One reason for the difference is that the actual contact area is smaller than this, and the other reason is that the threshold is expressed with "force" not "displacement." In airborne ultrasound tactile displays, the small force spot is effective at stimulating the skin at a low temporal frequency.

In comparison between 40 kHz and 70 kHz stimuli shown in Fig. 9, some subjects (Group A) showed comparable thresholds for 40 or 100 Hz modulations and other subjects (Group B) showed poorer sensitivity to the 40 kHz stimulus. A possible explanation is that FAII was the major (most sensitive) receptor in Group A, and SAI or

FAI was major in Group B. If a FAII receptor with a large receptive field is the main sensor, the threshold will show small dependence on the force area. If the main sensor is SAI or FAI with a small receptive area, force concentration will decrease the threshold expressed in the total force.

The result of Fig. 10(a) shows a relatively large dispersion. As a subjective comment by the authors, a localized pressure on the finger pad was clearly perceived. The reason for the dispersion came from ambiguity in how the subject understood the question. In the experiment, we just asked the subjects to answer the equivalence of the sphere size. This could have meant that the diameters of the radiation force area and the sphere are equivalent, or it could have also meant that the contact area between the finger and the ball was equivalent to the radiation force area. If the subject understood as the former, the equivalent diameter was small, and if it was the latter, the answered diameter become larger. It was the imperfectness of the experiment we noticed after the experiment. Nevertheless, we confirmed the subject could feel a localized force less than 1 cm in diameter on their finger pads.

7 Conclusions

A 70 kHz airborne ultrasound tactile display was fabricated and the effect of the higher spatial resolution was evaluated. The prototype display was composed of 91 transducers and its aperture diameter was 100 mm. In the physical experiment, we confirmed that the radiation force spot diameter of 70 kHz phased array was 43 % smaller than 40 kHz case at 150 mm from the device, comparing the foot width of the pressure distribution. The psychophysical experimental results showed that the minimum perceivable radiation force for the focal spot of 70 kHz was smaller than that for the 40 kHz case in average under 40 or 100 Hz modulations, and the smaller focal spot was easier to perceive. In the psychophysical experiments using the 70 kHz device, we obtained the detection thresholds for 40 Hz and 100 Hz vibrations. They are comparable, and the sensitivity difference was only 2 dB in the applied force. The subject could sense low frequency vibration easily, and perceived a localized sensation where the size could be compared with real objects.

Our future work includes representing fine texture in the tactile display. We will develop a fully controllable two-dimensional phased array.

References

1. Sodhi, R., Poupyrev, I., Glisson, M., Israr, A.: AIREAL: interactive tactile experiences in free air. ACM Trans. Graph. **32**(4), 134 (2013)
2. Iwamoto, T., Tatezono, M., Shinoda, H.: Non-contact method for producing tactile sensation using airborne ultrasound. In: Ferre, M. (ed.) EuroHaptics 2008. LNCS, vol. 5024, pp. 504–513. Springer, Heidelberg (2008)
3. Hoshi, T., Takahashi, M., Iwamoto, T., Shinoda, H.: Noncontact tactile display based on radiation pressure of airborne ultrasound. IEEE Trans. Haptics **3**(3), 155–165 (2010)

 4. Long, B., Seah, S.A., Carter, T., Subramanian, S.: Rendering volumetric haptic shapes in mid-air using ultrasound. ACM Trans. Graph. **33**(6), 181 (2014)
 5. Monnai, Y., Hasegawa, K., Fujiwara, M., Yoshino, K., Inoue, S., Shinoda, H.: Haptomime: mid-air haptic interaction with a floating virtual screen. In: Proceedings of the 27th Annual ACM Symposium on User Interface Software and Technology, pp. 663–667 (2014)
 6. Shinoda, H.: Haptoclone as a test bench of weak force haptic interaction. In: SIGGRAPH Asia 2015 Haptic Media and Contents Design, p. 3 (2015)
 7. Ishii, H., Ullmer, B.: Tangible bits: towards seamless interfaces between people, bits and atoms. In: Proceedings of the ACM SIGCHI Conference on Human Factors in Computing Systems, pp. 234–241 (1997)
 8. Asamura, N., Yokoyama, H., Shinoda, H.: Selectively stimulating skin receptors for tactile display. IEEE Comput. Graph. Appl. **18**(6), 32–37 (1998)
 9. Srinivasan, M.A., Dandekar, K.: An investigation of the mechanics of tactile sense using two-dimensional models of the primate fingertip. J. Biomech. Eng. **118**(1), 48–55 (1996)
10. Awatani, J.: Studies on acoustic radiation pressure. I. (General considerations). J. Acoust. Soc. Am. **27**(2), 278–281 (1955)
11. Hasegawa, T., Kido, T., Iizuka, T., Matsuoka, C.: A general theory of Rayleigh and Langevin radiation pressures. Acoust. Sci. Technol. **21**(3), 145–152 (2000)
12. Born, M., Wolf, E.: Principles of Optics: Electromagnetic Theory of Propagation, Interference and Diffraction of Light. CUP Archive, Cambridge (2000)
13. Gesheider, G.A., Bolanowski, S.J., Hardick, K.R.: The frequency selectivity of information-processing channels in the tactile sensory system. Somatosen. Mot. Res. **18**, 191–201 (2001)